Full length article

JHS(E)

The Journal of Hand Surgery
(European Volume)
0E(0) 1–13

DOI: 10.1177/1753193411432707
jhs.sagepub.com
SAGE

Subluxation-related ulnar neuropathy (SUN) syndrome related to distal radioulnar joint instability

P. S. C. Malone
Blond McIndoe Laboratories, University of Manchester; Department of Reconstructive Plastic Surgery, University Hospital South Manchester, Wythenshawe, UK

C. E. Hutchinson
Cancer and Enabling Sciences, University of Manchester, UK

N. S. Kalson
Department of Reconstructive Plastic Surgery, University Hospital South Manchester, Wythenshawe, UK

C. J. Twining
Imaging Science and Biomedical Engineering, University of Manchester, UK

G. Terenghi
Blond McIndoe Laboratories, University of Manchester, UK

V. C. Lees
Department of Reconstructive Plastic Surgery, University Hospital South Manchester, Wythenshawe, UK

Abstract
Ulnar neuropathy coexistent with distal radioulnar joint (DRUJ) instability has previously been observed in our practice. The aim of this study was to define this phenomenon and investigate the hypothesis that the cause of this intermittent, positional ulnar neuropathy is related to kinking of the ulnar nerve about the DRUJ. Ulna neuropathy was present in 10/51 (19.6%) of a historical cohort of patients who presented with DRUJ instability. Nine subsequent patients with DRUJ instability and coexistent ulnar neuropathy underwent 3-T magnetic resonance imaging to better understand the mechanism of the observed syndrome. Both 3D qualitative and quantitative analyses were used to assess the presence of nerve 'kinking', displacing the nerve from its normal course and causing nerve compression/distraction in the distal forearm and Guyon's canal. Results of the quantitative analysis were statistically significant ($p < 0.05$). The clinical features of the condition have been delineated and termed *subluxation-related ulnar neuropathy* or SUN syndrome. The imaging study was a level II diagnostic study.

Keywords
Distal radioulnar joint, DRUJ instability, triangular fibro cartilaginous complex (TFCC), ulnar neuropathy, MRI, SUN syndrome

Date received: 8th June 2011; revised 13th November 2011; accepted 20th November 2011

Introduction

Clinical observation of patients presenting with ulna-sided wrist pain and distal radioulnar joint (DRUJ) instability shows that some of them also have symptoms of ulnar neuropathy. Review of the literature

Corresponding author:
Miss V. C. Lees, Department of Plastic Surgery, University Hospital South Manchester, Wythenshawe Hospital, Southmoor Road, Manchester M23 9LT, UK
Email: vivienlees@live.com

Figure 1. MRI jig in use in the 3-T MRI scanner in the 'superman' position. Standard MR coils can be seen strapped to the wrist.

Box 1: Key Features of SUN Syndrome

- Ulnar neuropathy coincident with DRUJ instability
- Symptoms typically intermittent and related to forearm rotation
- Sensory symptoms predominate but can include intrinsic motor weakness
- Electrophysiology studies typically normal
- Pathogenesis is subluxation of the distal radius on the ulna head with associated distortion of the ulnar nerve proximal to Guyon's canal

clearly documents the link between ulnar nerve compression and ulnar neuropathy (Greene and Hadied 1981; Jose et al., 2006; Murata et al., 2003; Rengachary and Arjunan, 1981; Ruocco et al., 1998; Sakai et al., 2000; Shea and McClain, 1969). However, to our knowledge, only one previous reference suggests a causative link between DRUJ instability and ulnar neuropathy: Gong et al (2010) reported two cases of long-standing ulnar neuropathy associated with protrusion of the ulna head through a perforated volar joint capsule, precipitated by adjacent DRUJ synovitis and arthritis with associated ulnar neuritis. Surgical resolution of symptoms was achieved with resection of the ulna head, and it was considered to be a space-occupying lesion that was directly compressing the ulnar nerve.

Methods

Study design

Part 1 — historical cohort. An analysis of a historical cohort was completed to determine the incidence of ulnar neuropathy amongst a consecutive series of 51 patients referred to our services over a 2 year period with ulna-sided wrist pain and a final diagnosis of DRUJ instability. Diagnosis of the DRUJ instability was clinical, supported by magnetic resonance imaging (MRI) scans in most cases and confirmed at operation, in those cases that underwent surgical intervention. Some patients were given nonoperative treatment consisting of intensive physiotherapist-led wrist strengthening exercises to focus on development of the extensor carpi ulnaris, brachioradialis, pronator, and supinators. Ulnar neuropathy was diagnosed clinically and also with electrophysiology, in some cases. The features of the condition were delineated (see Box 1: Key Features).

Part 2 — image study cohort. A level II, diagnostic standard MRI study was undertaken on a further consecutive series of 9 patients who presented with DRUJ instability and had simultaneous ulnar neuropathy. Patients were recruited into the study for specialized MRI and informed consent obtained. Ethical permission was granted by the UK National Research Ethics Committee (reference number 07/Q1406/7). All patients were interviewed to assess their symptoms and, in particular, note any provoking factors, particularly the relationship of symptoms to forearm rotation. A clinical examination was undertaken to assess a range of pronosupination and note any features of sensory or motor involvement of the ulnar nerve. Ulnar nerve dysfunction was recorded according to standard criteria. Seven of the nine patients also underwent electrophysiology studies. Most of these patients also had intra-operative data to further substantiate the preoperative diagnosis of joint instability.

Imaging of the wrist joints

Plain radiographic series (posteroanterior [PA], lateral, 30° oblique, ulnar and radial deviation and power grip views) were obtained on all patients for both wrists. Bony abnormalities were assessed, in addition to noting any radiographic evidence of subluxation about the DRUJ. Ulnar variance and the type of sigmoid notch (Tolat et al., 1996) were both recorded, but numbers in each of the subgroups precluded meaningful analysis of the impact of joint conformation per se (Appendix I). Throughout the investigation, patients acted as their own case-controls in whom the contra-lateral wrist was symptom free.

High-resolution 3-T MRI scans (Philips Medical Systems, Eindhoven, Holland) were obtained with the use of a dedicated wrist coil. Patients were placed in the standard 'superman' position, as per current protocol for these scans. A specially constructed acrylic jig with an incorporated goniometer was also used (Figure 1). This jig held the wrist in the natural resting position (measured at 20.8° wrist dorsiflexion; SE over 20 measurements = 0.8°) whilst maintaining the wrist in a preselected position of forearm rotation, allowing the exact positioning to be reproduced for both intra- and inter-patient comparisons. The upper arm and antecubital fossa were strapped down to prevent rotation of the shoulder and elbow without compressing the soft tissues of the hand or forearm. The 3-T imaging sequence used was a proton density weighted image (PDW SPAI-SENSE, TR 4723 TE 8), with the long TR specifically used to better delineate the nerve. Scans of each wrist were obtained in maximal supination and pronation. Patients were specifically asked if any position of forearm rotation caused onset of their neurological symptoms, and a record was kept of any nerve-related symptoms experienced during the scans.

For each data series, 40 image slices were taken at 1 mm intervals from the level of the forearm, approximately 1 cm proximal to Guyon's canal through to the proximal pole of the pisiform, in order to delineate the position and conformation of discrete segments of the ulnar nerve in relation to bony landmarks. Avizo® v6.2 (Visualization Sciences Group, Bordeaux, France) was used for sequence stabilization to compensate for fine tremors and micromovements encountered during the scanning process.

Image analysis

For each wrist scanned, the ulnar nerve was identified and delineated through all 40 slices on each scan series in both maximal supination (SMax) and maximal pronation (PMax). SMax and PMax scans were compared to verify that the same structure had been isolated. The MR series for the contralateral arm was then analyzed alongside the scans on which the ulnar nerve had already been identified, flipping one image 180° horizontally so that the two were readily compared. The ulnar nerve was identified on the second wrist, and its course also tracked and delineated through each series of 40 scan images as for the first arm in both SMax and PMax. A consultant radiologist (author CEH) with a special interest in upper limb musculoskeletal imaging verified the accuracy of the ulnar nerve tracings.

Having identified and delineated the ulnar nerve, qualitative and quantitative analyses were undertaken in order to compare patients' affected wrists with their normal unaffected wrist (case-matched control).

Qualitative analysis: 2D and 3D reconstruction with analysis

Open-source image processing and DICOM workstation software, OsiriX® v3.1 32-bit (OsiriX Foundation, Geneva, Switzerland) was used to compare corresponding image series from patients' symptomatic and asymptomatic (control) wrists side-by-side. Images were co-registered by identifying the ulna fovea and then the sequences synchronized for scrolling purposes, allowing the course of the ulnar nerve to be tracked through the wrist in order to easily compare and contrast symptomatic and asymptomatic for identification of differences, abnormalities, and peculiarities on the 2D MR scans. In particular, it was noted whether the ulnar nerve on the abnormal wrist was displaced from its normal course, as defined by the route taken on the normal contra-lateral wrist. A combination of software programs were used. OsiriX® was used to continually refer back to and scroll through entire sequences to ensure accuracy and repeatability in delineating the course of the nerve. MRIcro® v1.40 (Chris Rorden, Atlanta, Georgia, USA) and Image Pro® Plus v6.2 (Media Cybernetics, Bethesda, Maryland, USA) were used to trace the bones, ulnar nerve, and ulnar artery through their course and to then reconstruct them through creation of a multiplanar 3D reconstruction. This was undertaken for all synchronized scan slices in series for both wrists of each patient in both SMax and PMax. The path of the ulnar nerve in relation to surrounding structures was then visually compared between normal and abnormal sides, and note taken of any differences in nerve course between the two wrists.

Quantitative analysis 1. Ulna:FCU interval measurements

At distal forearm level, the ulnar nerve lies between the flexor carpi ulnaris (FCU) tendon and head of the ulna. Findings of the qualitative analysis led us to measure and compare the length of the space between the FCU tendon and volar most aspect of the ulna head, which we termed the ulna:FCU interval. This measurement was performed using OsiriX® tools at the mid-level of the DRUJ corresponding to the ulna fovea. The length of the abnormal wrist was then taken as a denominator of the length of the normal wrist in order to draw correlations between the ulna:FCU interval and observed changes in the path of the ulnar nerve (Figure 2a, Table 2b). A Wilcoxon paired signed-rank test was undertaken to assess significance of the results.

Quantitative analysis 2 — deviation of polynomial from linear fit

Mathematical analysis was conducted (author CJT) across complete scan sequences to analyze the

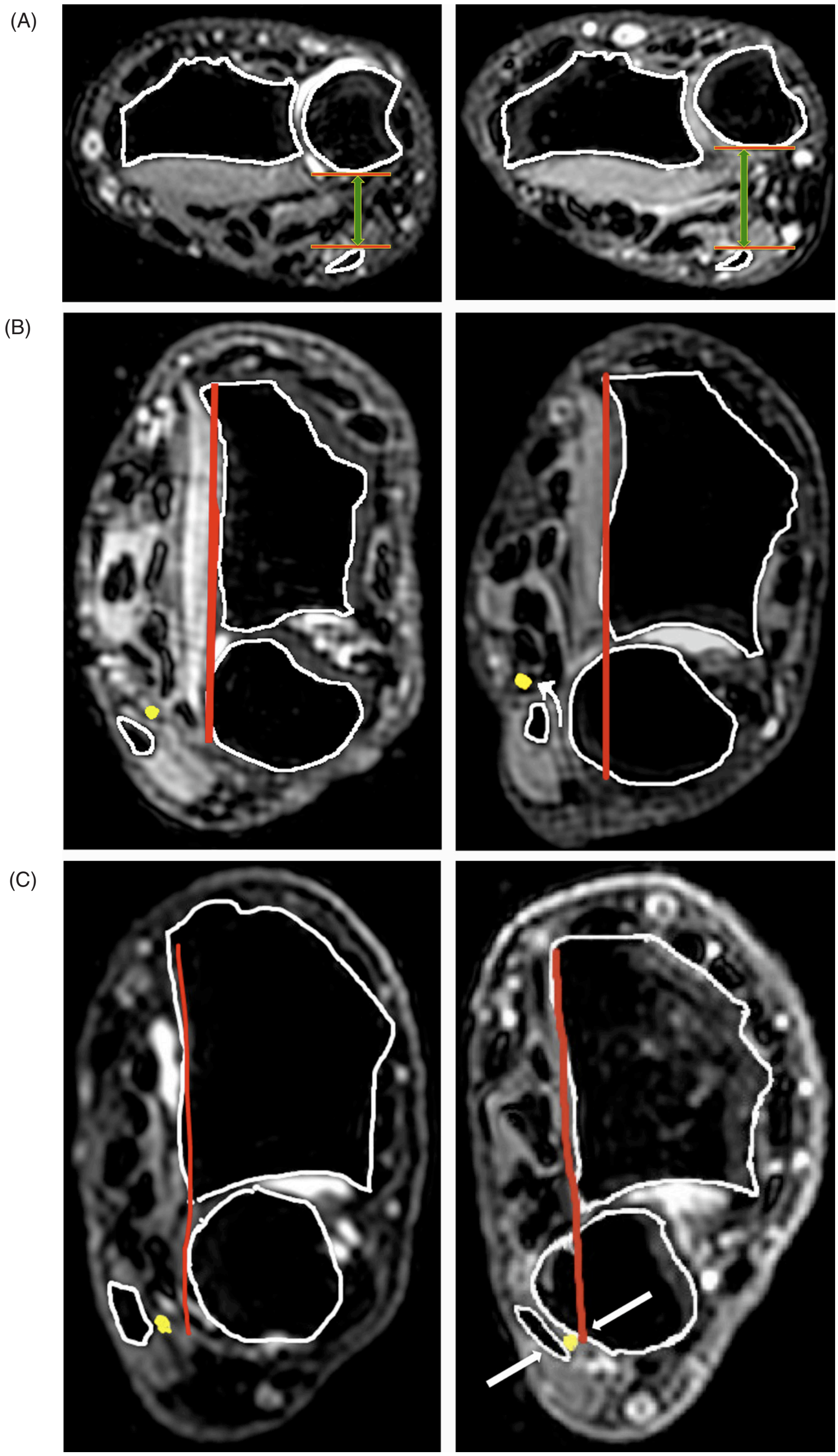

Figure 2. Axial MR scans through the distal radioulnar joint (DRUJ). Scans of the left wrist have been flipped 180° horizontally to allow direct side-by-side comparison. The ulna, radius, and flexor carpi ulnaris (FCU) tendon have all been delineated in white; the ulnar nerve in yellow. In (B) and (C). the red line depicts the volar border of the radius, with which the volar most border of the ulna head should be aligned. (A) Measurement of the ulna: FCU interval at the DRUJ; distance between the most dorsal point of the FCU tendon and volar-most point of the ulna head is measured. Image shown is patient 8 in Pmax, with the image on the right showing distraction as a result of volar subluxation of the distal radius. (B) MR scan of patient 1 in Smax: displacement of the ulna nerve is seen on the right associated with dorsal subluxation of the distal radius. (C) MR scan of patient 6 in Smax: compression of the ulna nerve is seen on the right associated with dorsal subluxation of the distal radius.

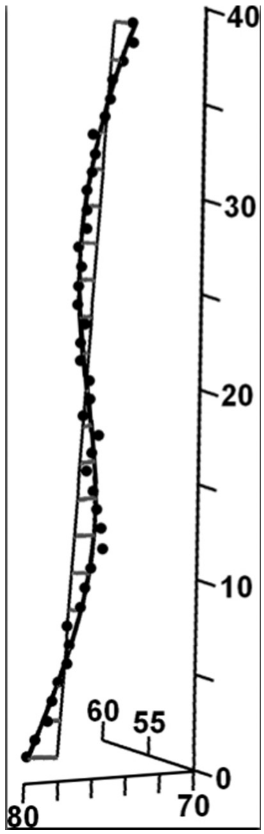

Figure 3. 3D modelling of the ulnar nerve: the ulnar nerve was traced across the sequence of 2D MR scans, its centre of mass computed, and then aligned nerve tracings were reconstructed to give a set of points in 3D. The nerve shown is of a symptomatic wrist. Units are in mm.

multidirectional variations in the 3D course of the ulnar nerve. To mathematically describe and quantify differences in the course of the ulnar nerve between both normal and abnormal wrists, the ulnar nerve was modelled to allow identification and analysis of any kinking, whether this was over a short or long segment of nerve. Images from one wrist were flipped 180° to allow direct comparison between left and right sides. A 3D track of the nerve was produced through computation of the centre of mass of the traced nerve regions on each image slice. The 2D slices were then reconstructed to produce a set of points in 3D representing the track of the nerve $\{(x_i, y_i, z_i)$: i = 1, to number of slices$\}$. An example is shown in Figure 3, where the z-axis represents the direction perpendicular to the plane of the slices.

The shape of the delineated nerve region was noted to vary between slices, in part due to branches from the nerve, thus leading to 'noise' when the centre of mass was extracted. To remove this effect, we produced a smoothed version of the track of the nerve. This was done by fitting a polynomial curve to the *x* coordinate as a function of *z*, and to the *y* coordinate as a function of *z*. That is:

$$x(z) = c_0 + c_1 z + c_2 z^2 + c_3 z^3 + \dots\dots\dots\ c_m z^m,$$

where m is the order of polynomial used (an example with $m = 7$ is shown in Figure 3). The coefficients $\{c_0, c_1, c_2, \dots, c_m\}$ were determined computationally by finding the values that gave the smallest difference between the fitted curve and original data points. A similar fitted curve was then constructed for $y(z)$, which then gave a single, continuous curve $\{x(z), y(z), z\}$, described by the $2m$ coefficients from the two fits.

To quantify the deviation of the smoothed estimate of the track of the nerve from a straight line, we also computed the best straight-line fit (that is, $m = 1$) to the set of points. We then sampled the smoothed estimate at a set of points equally spaced in *z*, and for each sample point, computed the shortest distance to the fitted straight line. The average of this over the set of samples then generated a single figure to quantify how far the curve deviated from a straight line. It is important to comment that a smoothed estimate was used for this measurement, because noisy samples from an actual straight line would give a non-zero value for the deviation, which would then be measuring the noise on the points, rather than the global deviation from a straight line. All computations were programmed in MATLAB R2006a (MathWorks Inc., Natick, Massachusetts, USA), using the Polyfitn tool (John D'Errico, www.mathworks.com/matlabcentral/fileexchange/10065-polyfitn). The magnitude of deviation of the ulnar nerve in abnormal wrists was compared with that of the track in the patient's normal wrist.

The assumption made in this analysis was that in healthy individuals, left and right sides do not usually differ. Thus, the null hypothesis was that there would be no deviation in the course of the ulnar nerve between a patient's symptomatic and asymptomatic sides. Wilcoxon paired signed-rank test was used to assess significance of the results, with $p < 0.05$ denoted to imply significance.

Results

Part 1 – historical cohort

Case note review of a consecutive series of patients referred over a 2 year period (2004–2006) identified a 20% (10/51 patients) incidence of ulnar neuropathy thought to be attributable to DRUJ instability (Table 1). Six patients had a history of prior wrist trauma. All

Table 1. Part 1 of study — symptomatic historical cohort: patient demographics, diagnoses, investigations, and treatments

Patient	Age, y	Duration of symptoms, y	Intermittent sensory symptoms	Motor symptoms	Nerve conduction studies	Intervention performed	Symptoms resolved
1	48	4	Y	N	Normal	TFCC reattachment	Y
2	33	4	Y	N	Not done	TFCC reattachment	Y
3	40	2	Y	Y	Normal	Ulna shortening	Y
4	56	2	Y	N	Normal	Ulna shortening	Y
5	63	3	Y	N	Not done	Bower's hemiresection interpositional arthroplasty	Y
6	60	7	Y	N	Not done	Bower's hemiresection interpositional arthroplasty	Y
7	32	4	Y	N	Normal	Physiotherapy only	Y
8	44	10	Y	N	Normal	Physiotherapy only	Y
9	19	7	Y	N	Lost to follow-up	Physiotherapy only	–
10	56	10	Y	N	Lost to follow-up	–	–

–, no data; TFCC, triangular fibro cartilage complex

patients indicated that they tried to avoid wrist positioning that brought on symptoms of ulnar neuropathy. Diagnosis of DRUJ instability was made by the senior author (VCL) and supported by findings from radiological investigations and definitive surgery. The clinical features of this condition are enumerated in Table 1.

The average age of symptomatic patients was 43.6 years (range 32–63). Ulnar nerve symptoms had an average duration of 5 years (range 2–10) were consistently both sensory and intermittent (10/10 patients), with additional motor symptoms in 1/10. Five patients attended for nerve conduction studies, and these were all normal. Six patients underwent DRUJ-stabilizing surgery without ulnar nerve decompression, and all had resolution of their symptoms of ulnar neuropathy. Two patients were treated solely with nonsurgical management through focussed physiotherapy wrist-strengthening exercises. Clinical assessment by the senior author (VCL) demonstrated improved DRUJ stability in both patients, accompanied by resolution of their symptoms of ulnar neuropathy. Two patients did not re-attend hospital after their initial consultations, and so were subsequently discharged. Of note, it was often documented that ulnar nerve sensory symptoms were not mentioned spontaneously, but only elicited by direct questioning. When three of the patients were directly asked why this was so, the reason expressed by each for omitting these symptoms was because they felt that the symptoms of tingling and paraesthesiae were relatively minor in the context of the other symptoms of DRUJ instability for which they were referred.

Part 2 — image study cohort

A subsequent cohort of 9 consecutive patients, mean age 40.7 years (range 27–55), who had a clinical diagnosis of DRUJ instability and ulnar neuropathy, with average duration of symptoms of 5 years (range 6 months – 20 years), were recruited for the imaging study. (A breakdown of patient demographics and key clinical findings is given in Table 2a.) One patient could only undertake scanning on the symptomatic side due to metalwork in the contralateral wrist. All patients had a history of prior wrist trauma and were subsequently clinically diagnosed as having DRUJ instability. The clinical diagnosis was supported by findings from radiological investigations, diagnostic wrist arthroscopy, or definitive surgery. Eight patients had intermittent symptoms of ulnar neuropathy, the ninth complained of a more constant paraesthesiae. Factors that provoked nerve-related symptoms included forearm rotation, with a predominance of symptoms specifically brought on by supination and by loading manoeuvres with the forearm in that position. All patients had sensory symptoms, but only three had coexistent motor involvement. Duration of symptoms had no correlation with actual symptomatology induced. Eight of the nine patients attended consultant-led nerve conduction studies, and all were reported as normal with no evidence of motor or sensory abnormality in the ulnar nerve. One patient underwent DRUJ-stabilizing surgery (without ulnar nerve decompression) prior to attending for electrophysiology, with resultant complete resolution of symptoms.

Table 2a. Image study cohort: Patient demographics, diagnoses, investigations and treatments

Patient	Age, y	Duration of symptoms, y	Positions of numbness	Motor symptoms	Nerve conduction studies	Intervention performed	Symptoms resolved
1	55	20	P30-SMax	Y	Normal	TFCC reattachment	Y
2	50	9	P30-SMax	N	Normal	Lost to follow up	–
3	30	2	S30-SMax	N	Not done	TFCC reattachment	Y
4	35	6	All	Y	Normal	TFCC reattachment	Y
5	34	4	All	N	Normal	Physiotherapy	Improved
6	52	2	All	N	Not done	Ulna shortening	Y
7	28	6 months	S30-SMax	Y	Normal	Physiotherapy	Y
8	27	3	All except neutral	N	Normal	TFCC reattachment	Y
9	55	2	PMax	N	Normal	TFCC reattachment	Y

–, no data; TFCC, triangular fibro cartilage complex.

Table 2b. Image study cohort: pronosupination range and qualitative analysis results from MR study investigations

Patient	Total range of rotation (pronation / supination)		Qualitative analysis Appearance of symptomatic nerve from both MRI transverse slices and 3D reconstructions
	Normal wrist	Abnormal wrist	
1	158 (70/90)	156 (66/90)	Displaced
2	134 (70/64)	124 (80/44)	Displaced
3	152 (64/88)	136 (54/82)	Displaced
4	160 (84/76)	156 (82/74)	Displaced
5	162 (72/90)	144 (72/72)	Displaced
6	154 (68/86)	140 (60/80)	Compressed
7	150 (62/88)	114 (72/42)	Distracted
8	142 (70/72)	130 (66/64)	Distracted
9	160 (84/76)	132 (74/58)	Compressed

Table 2c. Image study cohort: quantitative analysis results from MR study investigations

Patient	Quantitative analysis 1. Ulna:FCU interval (abnormal as ratio of normal)		Quantitative analysis 2. Deviation of polynomial from linear fit (abnormal as ratio of normal)	
	SMax	PMax	SMax	PMax
1	0.5	0.3	3.2	1.0
2	0.7	0.9	1.4	0.5
3	0.5	0.6	0.4	0.2
4	0.9	0.8	0.4	0.3
5	0.8	1.1	0.4	0.3
6	1.1	0.3	0.6	0.2
7	1.0	0.8	0.5	0.5
8	1.0	1.3	0.3	0.3

No data available for patient 9, as asymptomatic wrist previously plated for fracture.

During the MR data acquisition process, eight patients became symptomatic with ulnar nerve paraesthesiae without loading, whilst their wrist was held in the maximally supinated scanning position. Four patients also experienced paraesthesia in the maximally pronated scanning position. One patient did not develop any signs of ulnar nerve paraesthesiae whilst being assessed. No patients developed

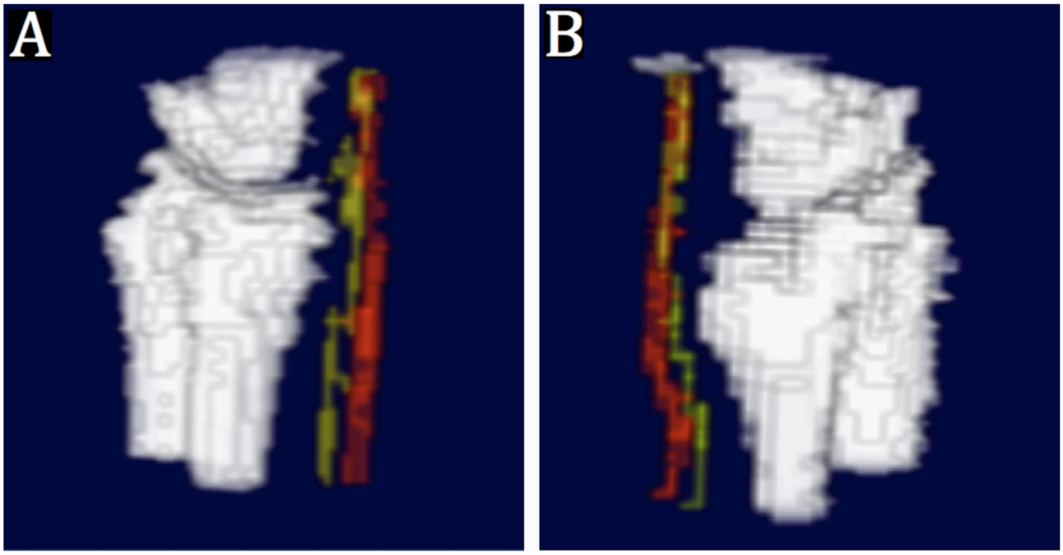

Figure 4. 3D reconstructions of the ulna nerve (yellow), artery (red), and bones (white) about the DRUJ of patient 5 in the asymptomatic (A) and symptomatic (B) wrists, held in Smax. A kink in both the ulna nerve and artery proximal to the DRUJ can clearly be seen on the symptomatic wrist. (Images were not smoothed with automatic computer interpolation in order to ensure that they remained true, accurate reconstructions of the wrist.)

symptoms in their asymptomatic limb. Post-operative consultant follow-up identified that of the 6 patients operated on to stabilize their DRUJ, all had complete resolution of neurological symptoms. No nerve decompression was undertaken at surgery. Of the three patients not operated on, two had improvement of their ulnar neuropathy symptoms with nonoperative management through physiotherapist-guided wrist strengthening exercises, combined with an avoidance of precipitating factors (one of these had complete resolution). DRUJ stability improved in both of these patients as assessed by the senior author (VCL). One patient did not re-attend clinic and her symptoms persisted, although she states they have improved with avoidance of aggravating factors.

PA radiographs showed some discrepancy in ulnar variance between symptomatic and asymptomatic wrists, although no general trends were identified (Appendix I). The majority of patients had a type II sigmoid notch slope, as per Deshmukh et al's classification (2000). Analysis of the nice patients' axial MR scans correlated with Tolat et al's DRUJ classification of 1996 as follows: three type A, three type B, two type C, and one type D. No correlation was noted between clinical symptoms and either of the DRUJ classifications.

Qualitative analysis

The image analysis described in the previous section was employed to isolate and track the ulnar nerve through individual scan slices for both normal and abnormal wrist, correlating nerve position with DRUJ alignment. All asymptomatic wrists had good bony alignment with no evidence of malalignment of either bones or the ulnar nerve. Qualitative analysis of the symptomatic wrists has been grouped to show two different resultant patterns identified when compared with the contra-lateral asymptomatic sides: ulnar nerve kinking and ulnar nerve compression/distraction. Results are shown in Table 2b, alongside measurements of range of pronosupination.

1. Ulnar nerve kinking

Alteration of the anatomical course of the ulnar nerve was observed in 5 out of 9 patients. The ulnar nerve deviated from its regular course in the distal forearm and Guyon's canal about the level of the DRUJ; this was evident on both MR scans (Figure 2b) and 3D reconstructions (Figure 4). MR scans revealed an obvious dorsal subluxation of the distal radius and radial displacement of the ulnar nerve. In the 3D reconstructions, a displacement in both the ulnar nerve and artery on the symptomatic side was identifiable, in contrast to the relatively straight course that they took on the other side. The 'kink' was located just proximal to the anatomical origin of Guyon's canal. Ulnar nerve displacement and kinking was more pronounced in SMax, but was also evident in PMax, albeit to a lesser degree. The average SMax for the symptomatic side was 73° (range 44–92°) compared with 81° (range 64–90°) for the asymptomatic side.

The average PMax was 68° (range 60–74°) compared with 71° (range 62–84°) for the asymptomatic side.

2. Ulnar nerve compression/distraction

Ulnar nerve compression and distraction were seen in four out of nine patients, associated with subluxation of the distal radius about the DRUJ. Two out of nine patients demonstrated a compressed space between the FCU and ulna head (termed compression). Where compression occurred, the ulnar nerve remained in anatomical alignment on the axial MR scans, but the space occupied was noted to be much reduced proximal to Guyon's canal (Figure 2c). In the other two patients, there was a widening of the space between the FCU and ulna head (termed distraction) associated with a subluxation of the distal radius (volar in one case, dorsal in the other). The radiocarpal ligaments and other radial-sided soft tissues of the wrist remained aligned with the distal radius, whereas the ulnar-sided tissues (including the ulnar nerve) were collectively deviated from their normal orientation as they crossed from the forearm to the hand. The average SMax for this subgroup was 61° (range 60–74°) compared with 81° (range 62–84°) for the asymptomatic side. The average PMax was 68° (range 42–80°) compared with 71° (range 72–88°) for the asymptomatic side. The reduction in supination for the 'distraction' group was less marked than that for the 'compression' group.

Quantitative analysis 1 — ulna:FCU interval analysis (n = 8)

Ulnar nerve displacement and 'compression/distraction' was seen to be due to a shift of the distal radius relative to the ulna head. Attributable to this shift, the dimensions of the space between the ulna head and FCU tendon (the ulna:FCU interval) were noted to be either reduced or enlarged compared with the normal side (Figure 2a). As shown in Table 2c, in patients 1–7, measurements consistently showed 20% or greater compression of this soft tissue space in either PMax or SMax, or both positions. In patient 8 (for whom distraction of the ulnar nerve was noted), the analysis of the MR scans depicted a volar shift of the distal radius in PMax with a corresponding 30% increase in the ulna:FCU interval on the symptomatic side. Measurements to compare the ulna:FCU interval were not possible in the normal wrist of patient 9 due to metalwork preventing MR scan acquisition on the normal wrist. Wilcoxon signed-ranks test gave a p value of 0.063 (not significant) for SMax and p = 0.036 for PMax ($p < 0.05$). This quantitative analysis of the ulna:FCU interval further supports the findings described in the qualitative analysis.

Quantitative analysis 2 — deviation of polynomial from linear fit (n = 8)

The findings of the first quantitative analysis raised the question of whether or not the differences between symptomatic and asymptomatic instances could be further compared using the track of the ulnar nerve in 3D space alone. To this end, the polynomial fitting and deviation-from-linearity measurement procedure described in the methods section was applied. The results from this quantitative analysis are documented in Table 2c and show the ratios of the deviation from linearity fit of the abnormal compared with the normal wrists. The Wilcoxon signed-rank test gave a p value of < 0.005 for SMax and $p < 0.005$ for PMax.

Discussion

This paper has detailed the phenomenon of ulnar neuropathy associated with DRUJ instability, and we have coined the term *subluxation-related ulnar neuropathy* or SUN syndrome to describe the observed clinical findings. The ulnar neuropathy observed is not typical of the compressive neuropathy of cubital tunnel syndrome, nor entrapment in Guyon's canal from the more usual causes. Rather, it is typically intermittent in nature, related to forearm rotation, predominantly sensory, is associated with negative electrophysiology, and resolves with treatment of the underlying instability. The incidence of SUN syndrome was relatively high, at approximately 20% in a patient cohort with final diagnosis of DRUJ instability in the first part of our study. Absence of symptoms in 80% of study patients is in keeping with variable expression of biological phenomena and may be related to underlying anatomical differences such as the length of the ulna. In the second part of the study, we used MRI techniques to investigate the possible causes of the syndrome and provided some interesting causative evidence of anatomical alteration of the track and topography of the nerve that we propose is related to the relevant clinical features.

Diagnosis of SUN syndrome

The diagnosis of SUN syndrome is made on clinical grounds and in the context of DRUJ instability. Symptomatic patients frequently recall a history of prior trauma to the wrist or forearm. In the current study, all patients experienced the phenomenon without the need for loading and predominantly in the maximally supinated position, although some patients also experienced the symptoms of paraesthesiae in the maximally pronated position and gradations in-between. Symptoms are typically intermittent, and EMG studies show no abnormality of ulnar nerve function at either wrist or elbow level. Few patients experienced motor symptoms, but in reflection motor neurological symptoms are usually pathognomonic of a chronic nerve impingement, whereas the described phenomenon is intermittent: patients are frequently able to avoid symptoms by avoiding provoking manoeuvres. None of the patients in the imaging study cohort had documented motor changes on electrophysiological investigation, but this is not to say that the same might not be observed in more severe cases.

Ligamentous damage around the DRUJ can be difficult to confirm radiologically (Garcia-Elias and Folgar, 2006). This is perhaps why the incidence of untreated ligamentous damage is high. For example, following distal radius fracture Lindau et al (2000a; 2000b) have recently shown it to be present in as many as 35% (27 /76) of young patients, 1 year post-distal–radius fracture, with corresponding significant symptoms and morbidity as measured with Gartland and Wertley scores. It is clear that clinical and radiological assessment of injuries of the distal radius and DRUJ needs to be refined to improve clinical outcomes for this cohort of patients. In passing, we suggest that it may be helpful to ask the radius fracture patient about ulnar border tingling and numbness. Where present, this may be a helpful pointer to the presence of radius subluxation on the ulna head, i.e. ligamentous damage.

Pathophysiology

Shea & McClain (1969) classified compressive ulnar neuropathy into three types, depending on the level of compression in relation to Guyon's canal: Type I is a mixed motor and sensory deficit (compression just proximal to or within Guyon's canal); Type II is purely motor (isolated compression of the deep branch of the nerve); and Type III is purely sensory (compression to the superficial sensory branch of the nerve).

In most instances, compressive ulnar neuropathy is regarded as idiopathic (Murata et al., 2003). Secondary causation has been associated with a ganglion (McDowell and Henceroth, 1977), cyst (Bowers and Doppelt, 1979), lipoma (Sakai et al., 2000), tortuous ulnar artery (Jose et al., 2006), giant cell tumour (Rengachary and Arjunan, 1981), carpal bone pathology (Greene and Hadied, 1981), anomalous muscles (Ruocco et al., 1998), and fibrous bands (Kochhar et al., 1973). Also described is ulnar nerve palsy as a direct consequence of distal radius fracture or from DRUJ degeneration subsequent to prior distal radius fracture (Clarke and Spencer, 1991; Frykman and Joshi, 1977; Saitoh et al., 2000; Vance and Gelberman, 1978). SUN syndrome is caused by DRUJ instability and could be considered a Type I subgroup of Shea and McClean's classification: due to its intermittent nature, predominantly sensory.

Qualitative and quantitative data presented in this paper have provided evidence to support a causative pathophysiology of the phenomenon termed SUN syndrome, consisting of topographical variations in the course of the ulnar nerve about the wrist. These variations appear to be either alterations in the 3D track of the nerve and/or displacement of the soft tissue and bony structures related to the nerve (see Figures 2b,2c,4). The principal cause, as judged from the 2D and 3D analyses, is that there is a displacement in the normal path of the ulnar nerve, causing it to kink. This kink is frequently caused by stretching of the ulnar nerve over the ulna head, which is made more prominent volarly due to a dorsal shift of the distal radius. This is in support of theories by other authors hypothesizing that the nerve is under stress and stretched when coexistent with DRUJ instability, such as Aoki et al's (2005) assessment of ulnar nerve strain through describing mobility of the ulnar nerve. Aoki implies that if the ulnar nerve is to be strained, this is most likely to occur at the level of Guyon's canal. This is consistent with our data provided from the Image Analysis group suggesting the site of interest to be just proximal to Guyon's canal.

The other mechanism by which DRUJ instability causes the phenomenon of intermittent ulnar neuropathy is that, instead of compression of the space through which the nerve passes, there is distraction. In support of this, the dimensions of the ulna:FCU interval have been noted to vary between different positions of pronosupination with symptoms particularly corresponding to when the interval is smallest (see Tables 2a,c). Associated subluxation of the radius at the DRUJ is also clearly seen, as illustrated in Figure 2, again suggesting DRUJ instability as the probable cause.

Treatment

Importantly, optimal treatment should be directed toward the underlying pathology and does not require nerve decompression; all of the patients described in this paper who underwent DRUJ-stabilizing surgery had resolution of their ulnar nerve symptoms, despite the fact that surgery did not include ulnar nerve decompression or release. In direct contrast, all of the previously described ulnar neuropathies in the literature that are coexistent with disorders of the wrist have been said to be compressive and specifically cured by ulnar nerve decompression (Greene and Hadied, 1981; Jose et al., 2006; Murata et al., 2003; Ruocco et al., 1998; Sakai et al., 2000; Shea and McClain, 1969). Decompression is achieved by directly opening Guyon's canal. Gong et al (2010) conceived of the ulna head as a space occupying lesion impinging the ulnar nerve, necessitating removal of the ulna head in two cases with synovitis and arthritis. We do not advocate removal of the ulna head. SUN syndrome, as described in the current paper, does not require decompression of Guyon's canal, but is curable with treatment of the underlying causative pathology of DRUJ instability alone (Tables 1, 2a).

Naming the syndrome

The acronym SUN syndrome has been coined to encapsulate our hypothesis regarding the pathophysiology of the disorder. Inherent in the terminology is the concept of the subluxation of the distal radius on the ulna head. The acronym serves as a double-entendre, with historical reference to Galileo's 17th century declaration of the revolution of planets around the sun in the face of the received wisdom of the day that the sun revolved around the earth. In the forearm, for decades the radius was regarded as the bone around which the ulna rotated, a misconception that often justified the unfortunate surgical removal of the ulna head as a treatment modality. However, at the wrist, it is in fact the ulna (the 'fixed' bone of the forearm) about which everything else rotates, and not the other way round. Even now, texts too frequently refer to "subluxation of the ulna head," when really it is the radius that moves around the fixed point of the ulna. As the distal radius subluxes on the ulna head, there is distortion in the soft tissues about the radius and embedded amongst these tissues is the distal most segment of the ulnar nerve. The name should serve as a reminder of the correct nomenclature for movements of the forearm bones.

Study limitations

The decision was made to analyze scans only at the extreme positions of rotation (SMax/PMax). There was, therefore, some variation between patients on the absolute value of Smax and Pmax. This decision was justified on the grounds that these were the positions in which patients stated they experienced most of their symptoms. This makes sense anatomically—for joint subluxation is most likely in the extremes of rotation—when the centroid of contact of the ulna head with the sigmoid notch of the radius is typically least congruous on either the dorsal or volar lip (as in PMax and SMax, respectively), and so joint subluxation is more likely. This effect is magnified in the presence of ligamentous damage. The quantitative analyses used here are relatively complex and reflect technical limitations of current technologies to find a simpler means of demonstrating the same phenomenon.

It is acknowledged that a relatively small number of patients were included in the image cohort analysis. This represents a consecutive series of patients exhibiting features of DRUJ instability with ulnar neuropathy (not all patients who presented with DRUJ instability had SUN syndrome). Out of the nine patients, there was one who had metalwork in the contralateral wrist, and no scan was therefore obtained of the contralateral wrist precluding any of the imaging comparisons. Data from this patient therefore appears in Table 2a and rotation ranges as recorded in Table 2b only. Statistical analysis does, however, appear to show a real effect of the alteration in anatomical relationships of the nerves on the unstable DRUJs in this limited number of cases. It has not been entirely clear to us as investigators whether we are looking at aspects of one single phenomenon impacting the nerve, or whether we are seeing a multifactorial causation of SUN syndrome.

The research aim for this study was to determine whether or not evidence could be provided for the existence of subluxation related ulnar neuropathy, to characterize the syndrome, and to determine aspects of its pathophysiology. To this end, the study was successful. It is acknowledged that, had resources allowed, it would have been a useful adjunct to the study to undertake and analyze a second set of MRI scans after resolution of the symptoms of SUN syndrome to see if post-treatment the anatomical track and typographical relationships of the nerve had been corrected. Full characterization of the phenomenon, possibly using future technologies, should be possible, but was out of the limits of this particular study.

Acknowledgements

Dr W. A. Bhatti, Consultant Musculoskeletal Radiologist, University Hospital South Manchester, UK; TIU departmental team; Mr R. Williams, former Clinical Engineer, University Hospital South Manchester; Professor P. Williams, Research & Development Lead, Christie Hospital, Manchester; The Medical Engineering Department, Hope Hospital; Dr Sue Shawcross, Blond McIndoe Laboratories; and Julie Morris, Head of Medical Statistics, University Hospital South Manchester.

Patients were recruited into this study for specialised MR imaging through obtaining informed consent. Ethical permission was granted by the UK National Research Ethics Committee (reference number 07/Q1406/7).

Conflict of interests

None declared.

Funding

This research was supported by funding from the Stanley Thomas Johnson Foundation, University of Manchester MRC Interdisciplinary Bridging Award administered through the Manchester centre for the Integration of Medicine and Innovative Technology (MIMIT), and also the Transitional Imaging Unit (TIU), Salford Royal Hospital NHS Foundation Trust, UK.

References

Sachar K. Ulnar-sided wrist pain – evaluation and treatment of triangular fibrocartilage complex tears, ulnocarpal impaction syndrome, and lunotriquetral ligament tears. J Hand Surg Am. 2008: 1–11.

Aoki M, Takasaki H, Muraki T, Uchiyama E, Murakami G, Yamashita T. Strain on the ulnar nerve at the elbow and wrist during throwing motion. J Bone Joint Surg Am. 2005, 87: 2508–14.

Bowers WH, Doppelt SH. Compression of the deep branch of the ulnar nerve by an intraneural cyst. Case report. J Bone Joint Surg Am. 1979, 61: 612–3.

Clarke AC, Spencer RF. Ulnar nerve palsy following fractures of the distal radius: clinical and anatomical studies. J Hand Surg Br. 1991, 16: 438–40.

Deshmukh SC, Shanahan D, Coulthard D. Distal radioulnar joint incongruity after shortening of the ulna. J Hand Surg Br. 2000, 25: 434–8.

Frykman G. Fracture of the distal radius including sequelae—shoulder-hand-finger syndrome, disturbance in the distal radio-ulnar joint and impairment of nerve function. A clinical and experimental study. Acta Orthop Scand. 1967, (Suppl 108):1–155.

Garcia-Elias M, Folgar MAV. The management of wrist injuries: an international perspective. Injury. 2006, 37: 1049–56.

Gong HS, Kim KH, Roh YH, Lee YH, Chung MS, Baek GH. Delayed-onset ulnar neuropathy at the wrist associated with distal radioulnar joint arthritis after radius malunion: report of two cases. J Hand Surg Am. 2010, 35: 233–6.

Greene MH, Hadied AM. Bipartite hamulus with ulnar tunnel syndrome-case report and literature review. J Hand Surg Am. 1981, 6: 605–9.

Jose RM, Bragg T, Srivastava S. Ulnar nerve compression in Guyon's canal in the presence of a tortuous ulnar artery. J Hand Surg Br. 2006, 31: 200–2.

Joshi BB. An unusual cause of ulnar nerve palsy associated with Colles's fracture. Hand. 1977, 9: 76–8.

Kochhar VL, Man Singh J, Srivastava KK. Delayed ulnar nerve palsy in colles' fracture: a case report. Aust N Z J Surg. 1973, 43: 54–6.

Lindau T, Adlercreutz C, Aspenberg P. Peripheral tears of the triangular fibrocartilage complex cause distal radioulnar joint instability after distal radial fractures. J Hand Surg Am. 2000a, 25: 464–8.

Lindau T, Hagberg L, Adlercreutz C, Jonsson K, Aspenberg P. Distal radioulnar instability is an independent worsening factor in distal radial fractures. Clin Orthop Relat Res. 2000b: 229–35.

McDowell CL, Henceroth WD. Compression of the ulnar nerve in the hand by a ganglion. Report of a case. J Bone Joint Surg Am. 1977, 59: 980.

Murata K, Shih J-T, Tsai T-M. Causes of ulnar tunnel syndrome: a retrospective study of 31 subjects. J Hand Surg Am. 2003, 28: 647–51.

Rengachary SS, Arjunan K. Compression of the ulnar nerve in Guyon's canal by a soft tissue giant cell tumor. Neurosurg. 1981, 8: 400–5.

Ruocco MJ, Walsh JJ, Jackson JP. MR imaging of ulnar nerve entrapment secondary to an anomalous wrist muscle. Skeletal Radiol. 1998, 27: 218–21.

Saitoh S, Seki H, Murakami N, Hata Y, Takaoka K. Tardy ulnar tunnel syndrome caused by Galeazzi fracture-dislocation: a neuropathy with a new pathomechanism. J Orthop Trauma. 2000, 14: 66–70.

Sakai K, Tsutsui T, Aoi M, Sonobe H, Murakami H. Ulnar neuropathy caused by a lipoma in Guyon's canal-case report. Neurol Med Chir (Tokyo). 2000, 40: 335–8.

Shea JD, McClain EJ. Ulnar-nerve compression syndromes at and below the wrist. J Bone Joint Surg Am. 1969, 51: 1095–103.

Tolat AR, Stanley JK, Trail IA. A cadaveric study of the anatomy and stability of the distal radioulnar joint in the coronal and transverse planes. J Hand Surg Br. 1996, 21: 587–94.

Vance RM, Gelberman RH. Acute ulnar neuropathy with fractures at the wrist. J Bone Joint Surg Am. 1978, 60: 962–5.

Appendix I

Image study cohort: results of radiograph review

Patient	Ulnar variance, mm		Sigmoid notch slope type/ DRUJ angle (1–3) *(as per Deshmukh et a.l, 2000)*		Type of DRUJ(A = flat face sigmoid; B = ski slope sigmoid; C = C-type sigmoid; D = S-type sigmoid] *(as per Tolat et al., 1996)*	
	Normal wrist	Abnormal wrist	Normal wrist	Abnormal wrist	Normal wrist	Abnormal wrist
1	−0.6	3.3	2	2	B	B
2	−1.8	2.2	2	2	A	A
3	−0.8	0.0	2	2	A	A
4	0.0	0.0	2	2	D	D
5	−2.2	−2.0	2	2	D	C
6	−0.8	0.0	2	2	A	A
7	0.0	0.0	2	2	C	C
8	0.0	−0.4	1	2	B	B
9	−1.4	−2.3	2	2	–	B

–, No result (as no MR)